MOLECULAR AND CELLULAR BIOLOGY, Aug. 2009, p. 4527–4538 Vol. 29, No. 16
0270-7306/09/$08.00+0 doi:10.1128/MCB.00200-09
Copyright © 2009, American Society for Microbiology. All Rights Reserved.

Hypoxia-Inducible Factor 2 Regulates Hepatic Lipid Metabolism▽†

Erinn B. Rankin,[1]‡ Jennifer Rha,[1] Mary A. Selak,[2] Travis L. Unger,[1] Brian Keith,[3] Qingdu Liu,[1,4] and Volker H. Haase[1,4]*

Department of Medicine, University of Pennsylvania, Philadelphia, Pennsylvania[1]; Children's Hospital, University of Pennsylvania School of Medicine, Philadelphia, Pennsylvania[2]; Abramson Family Cancer Research Institute and Howard Hughes Medical Institute, University of Pennsylvania, Philadelphia, Pennsylvania[3]; and Department of Medicine, Cancer Biology, Molecular Physiology and Biophysics, Vanderbilt School of Medicine, Nashville, Tennessee[4]

Received 12 February 2009/Returned for modification 22 March 2009/Accepted 8 June 2009

In mammals, the liver integrates nutrient uptake and delivery of carbohydrates and lipids to peripheral tissues to control overall energy balance. Hepatocytes maintain metabolic homeostasis by coordinating gene expression programs in response to dietary and systemic signals. Hepatic tissue oxygenation is an important systemic signal that contributes to normal hepatocyte function as well as disease. Hypoxia-inducible factors 1 and 2 (HIF-1 and HIF-2, respectively) are oxygen-sensitive heterodimeric transcription factors, which act as key mediators of cellular adaptation to low oxygen. Previously, we have shown that HIF-2 plays an important role in both physiologic and pathophysiologic processes in the liver. HIF-2 is essential for normal fetal *EPO* production and erythropoiesis, while constitutive HIF-2 activity in the adult results in polycythemia and vascular tumorigenesis. Here we report a novel role for HIF-2 in regulating hepatic lipid metabolism. We found that constitutive activation of HIF-2 in the adult results in the development of severe hepatic steatosis associated with impaired fatty acid β-oxidation, decreased lipogenic gene expression, and increased lipid storage capacity. These findings demonstrate that HIF-2 functions as an important regulator of hepatic lipid metabolism and identify HIF-2 as a potential target for the treatment of fatty liver disease.

The liver plays a central role in maintaining overall organism energy balance by controlling carbohydrate and lipid metabolism. Hepatocytes coordinate these processes by regulating gene expression programs in response to dietary signals from the portal vein and systemic signals from the hepatic artery. Oxygen is an important systemic signal that modulates metabolic activities and disease in the liver. Under physiologic conditions, an oxygen gradient is established in the liver such that the partial pressure of oxygen in periportal blood is 60 to 65 mm Hg and in the perivenous blood is 30 to 35 mm Hg (17). This oxygen gradient is important for the zonation of metabolic activity in the liver. Because oxygen is an essential electron acceptor for oxidative metabolism, hepatocytes that perform glucose or fatty acid oxidation are located in the aerobic periportal zone, whereas oxygen-independent metabolic functions such as glucose uptake, glycolysis, and fatty acid synthesis are predominately performed by perivenous hepatocytes (16). Patients who experience perivenous hypoxia as a result of heart failure, obstructive sleep apnea, or excessive alcohol use can develop chronic liver injury characterized by steatosis and inflammation (17). Therefore, it is critical that oxygen-signaling pathways in hepatocytes are appropriately integrated into adaptive and/or maladaptive liver injury responses.

Hypoxia-inducible transcription factors (HIFs) are important components of the cellular oxygen-signaling pathway. In response to low oxygen tensions, HIFs facilitate both oxygen delivery and adaptation to oxygen deprivation by regulating the expression of genes that are involved in glucose uptake and metabolism, angiogenesis, erythropoiesis, cell proliferation, and apoptosis (45, 51). HIFs belong to the PAS (Per-ARNT-Sim) family of basic helix-loop-helix transcription factors that bind to DNA as heterodimers and are composed of an oxygen-sensitive α subunit and a constitutively expressed β subunit, also known as the arylhydrocarbon receptor nuclear translocator (ARNT). Three HIF-α subunits (HIF-1α, -2α, and -3α) have been identified and are targeted by the von Hippel-Lindau (VHL) tumor suppressor, pVHL, for ubiquitination and subsequent proteasomal degradation under normoxia. Loss of cellular pVHL function results in the stabilization of HIF-α subunits and constitutive activation of HIF signaling (29, 42).

The liver expresses all three HIF-α family members, HIF-1α, -2α, and -3α, under physiologic and pathophysiologic conditions, suggesting that HIFs are important mediators of normal liver function and disease. We recently reported that hepatic HIF-2 is required for fetal *EPO* production and erythropoiesis, while constitutive HIF-2 activation in the adult liver causes polycythemia and vascular tumorigenesis (35, 37). With regard to metabolism in the liver, HIF-1 regulates the expression of glucose transporters as well as glycolytic enzymes and is thought to contribute to the glycolytic phenotype of hepatocellular carcinomas (11, 36, 46). In addition, recent studies have suggested a role for HIF in the regulation of hepatic lipid

* Corresponding author. Mailing address: Department of Medicine, Division of Nephrology and Hypertension, Vanderbilt University Medical Center, C-3119A, MCN, 1161 21st Avenue, Nashville, TN 37232. Phone: (615) 343-7254. Fax: (615) 322-6854. E-mail: volker.haase@vanderbilt.edu.

† Supplemental material for this article may be found at http://mcb.asm.org/.

‡ Present address: Division of Cancer and Radiation Biology, Department of Radiation Oncology, Stanford University, CCSR-South, Room 1255, 269 Campus Drive, Stanford, CA 94305.

▽ Published ahead of print on 15 June 2009.

metabolism; however, the contributions of HIF-1 and/or HIF-2 in this process remain unclear (1, 10, 17, 49).

In order to investigate the functions of HIF-1 and HIF-2 in hepatic lipid metabolism, we utilized Cre-*loxP*-mediated recombination and inactivated Hif-1α or Hif-2α in the livers of pVHL-deficient mice. Genetic inactivation of the murine *VHL* gene, *Vhlh*, in hepatocytes results in constitutive activation of both Hif-1 and Hif-2 and is associated with the development of severe hepatic steatosis (36). Here, we report that, similarly to Vhlh-deficient mice, Vhlh/Hif-1α mutant mice developed severe steatohepatitis, which was associated with impaired fatty acid β-oxidation, decreased lipogenic gene expression, and increased lipid storage capacity. In contrast, inactivation of Hif-2α significantly suppressed the development of hepatic steatosis, indicating a novel role for HIF-2 in the regulation of hepatic lipid metabolism in vivo. Our results suggest that HIF-1 and HIF-2 have unique roles in the metabolic adaptation to hypoxia, and more importantly, they identify HIF-2 as a potential target for the treatment of fatty liver disease.

MATERIALS AND METHODS

Generation and analysis of mice. The generation of *Vhlh*, *Hif-1α*, and *Epas1* (*Hif-2α*) conditional alleles and albumin-Cre and PEPCK-Cre transgenes has been previously described (8, 10, 34, 38, 41). Cre-mediated inactivation of *Vhlh*, *Hif-1α*, and *Hif-2α* in hepatocytes was accomplished by generating mice that were homozygous for the respective 2-lox alleles and expressed the albumin-Cre or the PEPCK-Cre transgenes. Littermates not carrying the Cre transgene were used as control animals. Mutant mice were generated in a mixed genetic background (BALB/c, 129Sv/J, and C57BL/6). The primer sequences used to detect the nonrecombined (2-lox), recombined (1-lox), and wild-type alleles for *Vhlh*, *Hif-1α*, and *Hif-2α* have been previously described (8, 36). All procedures involving mice were performed in accordance with the National Institutes of Health guidelines for use and care of live animals and were approved by the Institutional Animal Care and Use Committee.

Protein isolation and Western blot analysis. Nuclear and cytoplasmic protein extracts were prepared and analyzed by Western blotting as previously described (36). Primary antibodies for Western blot analysis included a polyclonal actin (Sigma-Aldrich), polyclonal acetyl coenzyme A (CoA)-carboxylase Ser 79 (Cell Signaling), phosphoacetyl-CoA-carboxylase Ser 79 (Cell Signaling), and adipose differentiation-related protein (RDI Division of Fitzgerald Industries International).

RNA isolation and reverse transcription-PCR. RNA was isolated using the RNeasy maxikit according to the manufacturer's protocols (Qiagen Inc.). cDNA was synthesized from 4 μg of DNase (Invitrogen)-treated RNA using the SuperScript first-strand synthesis system for reverse transcription-PCR (Invitrogen). One microliter of cDNA was subjected to PCR amplification using either SYBR green PCR Master Mix or TaqMan Universal PCR Master Mix (Applied Biosystems). The primer and probe sets used to amplify specific target genes can be found in Fig. S1 in the supplemental material. TaqMan primers for 18S were previously published (36). PCR amplification was performed on the ABI Prism 7300 sequence detection system (Applied Biosystems) as previously described (36). 18S was used to normalize mRNA. The relative standard curve method was used for quantitation of mRNA expression levels according to the manufacturer's instructions (Applied Biosystems).

RNA interference studies. HepG2 and RCC4 cells were transfected with control, *HIF-1α*, *HIF-2α*, or *ARNT* small interfering RNA (siRNA) oligonucleotides using the HiPerFect (Qiagen Inc.) and Dharmafect 1 (Dharmacon) transfection reagents according to the manufacturer's protocols (Qiagen Inc. and Dharmacon). Forty-eight hours after transfection, hypoxic samples were exposed to 1 or 0.5% oxygen for 18 h. The following siRNA oligonucleotides were purchased through Qiagen's prevalidated siRNA database: *ARNT* siRNA target sequence, GAAGUCAGAUGGUUUAUUU; *HIF-1* HP validated siRNA, catalog no. SI02664053; *HIF-2* HP validated siRNA, catalog no. SI02663038. Control siRNAs were purchased from Dharmacon siGENOME nontargeting siRNA pool 2 (D0012061405). For Fig. S3A in the supplemental material, *HIF-1*, *HIF-2*, and *ARNT* siRNA oligonucleotides were purchased from Dharmacon ON-TARGETplus siRNA pools.

Metabolic characterization. Serum glucose, triglycerides, and nonesterified fatty acids were measured using enzymatic assays following the manufacturer's protocols (Stanbio). Serum liver chemistry assays including those for aspartate transaminase, alanine aminotransferase, alkaline phosphatase, bilirubin, and albumin were performed by the University of Pennsylvania Clinical Lab using standard procedures. Liver triglyceride concentrations were determined by enzymatic assays according to the manufacturer's protocols (Stanbio no. 2150). For total liver lipid analysis, lipids were extracted from livers in the presence of authentic internal standards by the method of Folch et al. (6) using chloroform-methanol (2:1, vol/vol). Individual lipid classes within each extract were separated by liquid chromatography (Agilent Technologies model 1100 series). Each lipid class was transesterified in 1% sulfuric acid in methanol in a sealed vial under a nitrogen atmosphere at 100°C for 45 min. The resulting fatty acid methyl esters were then extracted from the mixture with hexane containing 0.05% butylated hydroxytoluene and prepared for gas chromatography by sealing the hexane extracts under nitrogen. Fatty acid methyl esters were separated and quantified by capillary gas chromatography (Agilent Technologies model 6890) equipped with a 30-m DB-88MS capillary column (Agilent Technologies) and a flame ionization detector.

Immunohistochemical analysis. Livers were fixed overnight in 10% phosphate-buffered formalin, processed for routine embedding in paraffin, and cut 6 μm in thickness onto glass slides. Slides were dewaxed in xylene and rehydrated through graded ethanol washes. Hematoxylin and eosin staining was performed using standard procedures. For Adfp staining, frozen tissue sections were stained with the Adfp antibody at 1:1,000 overnight (Fitzgerald) followed by incubation with the secondary Cy3-labeled donkey anti-guinea pig antibody (Vector Laboratories). For Oil Red O staining, frozen tissue sections were stained in 0.5% Oil Red O in propylene glycol overnight and counterstained with hematoxylin. Nile red staining was performed as previously described (7).

Microarray expression profiling and data analysis. Microarray expression profiling and data analysis were essentially performed as previously described (52) with the following exceptions: 20 μg of total RNA isolated from the livers of 3-week-old albumin-Vhlh/Hif-1α, albumin-Vhlh/Hif-2α, and albumin-Vhlh/Hif-1α/Hif-2α mutant mice was used in the array hybridization. A common control RNA sample was comprised of a mixture of RNAs taken from all samples.

Polarographic measurement of oxygen consumption. Oxygen consumption of liver mitochondria was measured using a Strathkelvin oxygen electrode in a magnetically stirred, thermostatically regulated chamber (30°C). Approximately 1 mg mitochondrial protein was suspended in a total volume of 0.15 ml of air-saturated buffer composed of 220 mM mannitol, 70 mM sucrose, 5 mM HEPES (pH 7.2), 5 mM KH_2PO_4, and 0.1 mM EGTA. Oxidation of carnitine esters was measured in the presence of 2 mM malate and 1 mM $MgCl_2$ with 0.05 mM palmitoylcarnitine, 0.2 mM octoylcarnitine, or 1 mM acetylcarnitine followed by addition of 0.2 mM ADP. Oxygen consumption was also measured without the addition of carnitine esters in the presence of 10 mM glutamate plus 2 mM malate or 10 mM succinate plus 2 μM rotenone. Rates of substrate oxidation with or without ADP were expressed as nanoatoms of oxygen consumed per minute per milligram mitochondrial protein. State 3 refers to oxygen consumption stimulated by a limiting amount of ADP, as opposed to state 4, which refers to oxygen consumption after phosphorylation of the added ADP to ATP.

Statistical analysis. Statistical analysis was performed using the unpaired Student *t* test. *P* values of <0.05 were considered statistically significant.

RESULTS

Generation and characterization of albumin-Vhlh, -Vhlh/Hif-1α, -Vhlh/Hif-2α, and -Vhlh/Hif-1α/Hif-2α mutant mice. We recently reported that conditional inactivation of the tumor suppressor *Vhlh* in hepatocytes results in the development of severe hepatic steatosis associated with constitutive activation of Hif-1 and Hif-2 (10, 36). To determine the requirement for Hif-1 and Hif-2 in the development of hepatic steatosis, we utilized the albumin-Cre transgenic line to inactivate Hif-1α or Hif-2α in *Vhlh*-deficient mice. For this purpose, albumin-Cre transgenic mice were bred to mice homozygous for either the *Vhlh*; *Vhlh* and *Hif-1α*; *Vhlh* and *Hif-2α*; or *Vhlh*, *Hif-1α*, and *Hif-2α* conditional alleles to generate the following mutant mice: $Vhlh^{2lox/2lox}$; *Albumin-Cre*, $Vhlh^{2lox/2lox}$ $Hif\text{-}1\alpha^{2lox/2lox}$;

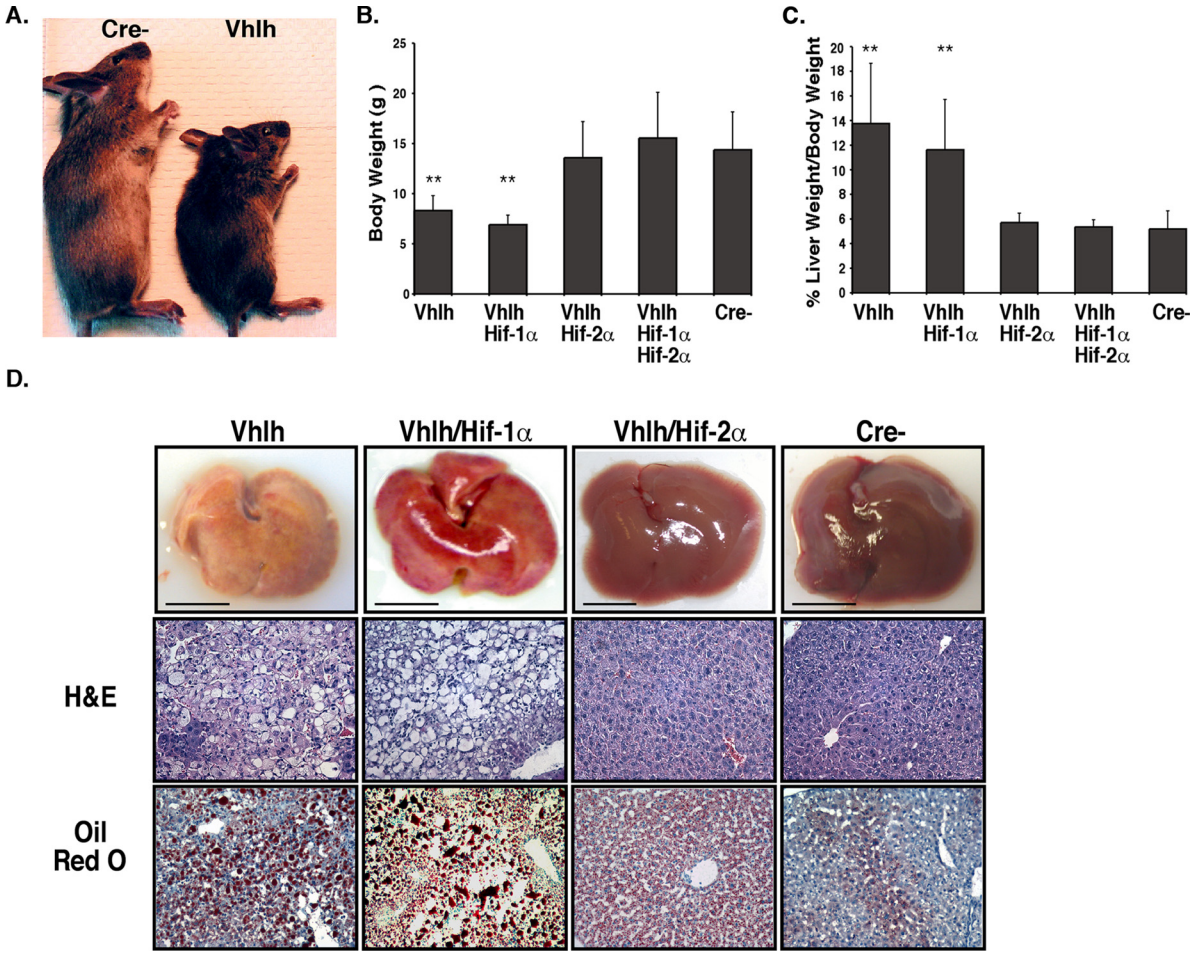

FIG. 1. Inactivation of Hif-2α suppresses the development of hepatic steatosis in albumin-Vhlh mutant mice. (A) Photograph of 4-week-old control (Cre^-) and albumin-Vhlh mutant mice. (B) Average body weights of albumin-Vhlh, -Vhlh/Hif-1α, -Vhlh/Hif-2α, -Vhlh/Hif-1α/Hif-2α, and control (Cre^-) mice. (C) Percent liver weight to body weight in albumin-Cre mutant mice. For panels B and C, asterisks indicate a significant difference in body weight or in liver-to-body weight ratio from that of control (Cre^-) mice (**, $P < 0.001$) as determined by the Student *t* test. (D) Macroscopic and histological analysis of albumin-Cre mutant livers. Note the pale color of the albumin-Vhlh and -Vhlh/Hif-1α mutant livers (top row). Bars, 7 mm. Hematoxylin and eosin (H&E) and Oil Red O staining show neutral lipid accumulation in large macrovesicular lipid droplets found in albumin-Vhlh- and -Vhlh/Hif-1α-deficient livers.

Albumin-Cre, *Vhlh*$^{2lox/2lox}$ *Hif-1α*$^{2lox/2lox}$; *Albumin-Cre*, and *Vhlh*$^{2lox/2lox}$ *Hif-1α*$^{2lox/2lox}$ *Hif-2α*$^{2lox/2lox}$; *Albumin-Cre* mice, hereafter referred to as albumin-Vhlh, albumin-Vhlh/Hif-1α, albumin-Vhlh/Hif-2α, and albumin-Vhlh/Hif-1α/Hif-2α mutants, respectively. Albumin-Cre transgenic mice express Cre recombinase in the majority of hepatocytes (>80%) and mediate efficient recombination of the *Vhlh*, *Hif-1α*, and *Hif-2α* conditional alleles, resulting in complete loss of Hif-1α and Hif-2α protein in albumin-Vhlh/Hif-1α/Hif-2α mutant mouse livers (34).

Albumin-Vhlh, -Vhlh/Hif-1α, -Vhlh/Hif-2α, and Vhlh/Hif-1α/Hif-2α mutant mice were born at expected Mendelian ratios (data not shown). By postnatal day 6, albumin-Vhlh mutants differed from wild-type mice by a 23.5% reduction in average body weight and pale yellow livers (data not shown). At day 28, both albumin-Vhlh and Vhlh/Hif-1α mutant mice were readily distinguishable from their Cre^- littermates by significantly reduced size and body weight (Fig. 1A and B) and pale yellow livers that were enlarged twofold (Fig. 1C and D). Histological examination of albumin-Vhlh and -Vhlh/Hif-1α mutant mouse livers revealed severe steatohepatitis. The cytoplasm in >90% of hepatocytes was weakly eosinophilic and contained large macrovesicular vacuoles that displaced nuclei toward the cell periphery (Fig. 1D). Oil Red O staining revealed that macrovesicular vacuoles in albumin-Vhlh and -Vhlh/Hif-1α mutant mice contained neutral lipids that were associated with an 18.2-fold increase in hepatic triglyceride content (Fig. 1D and Table 1). The development of hepatic steatosis in albumin-Vhlh and -Vhlh/Hif-1α mutants was associated with shortened life spans and morbidity between ages 4 and 8 weeks (data not shown). Strikingly, albumin-Vhlh/Hif-2α mutant mice were phenotypically normal and appeared similar to wild-type or albumin-Vhlh/Hif-1α/Hif-2α mutant mice upon macroscopic evaluation (Fig. 1B, C, and D). Histologically, we observed an increase in the number of hepatocytes with microvesicular lipid accumulation that resulted in a 2.2-fold increase in hepatic triglyceride content compared to control mice (Fig. 1D and Table 1).

TABLE 1. Metabolic characterization of albumin-Cre mutant mice

Serum or liver chemical (unit of measure)[a]	Mean ± SEM for mouse type[b]:				
	Vhlh	Vhlh/Hif-1α	Vhlh/Hif-2α	Vhlh/Hif-1α/Hif-2α	Cre⁻
Serum					
Liver function (n = 4)					
AST (U/liter)	314 ± 99*	303 ± 53*	115 ± 13	93 ± 21	96 ± 3
ALT (U/liter)	47 ± 7	63 ± 10	58 ± 4	57 ± 5	48 ± 3
ALP (U/liter)	804 ± 111*	1,246 ± 125**	350 ± 44	255 ± 40*	389 ± 16
Bilirubin, total (mg/dl)	10 ± 2**	8.5 ± 4*	0.4 ± 0.2	0.18 ± 0.05	0.15 ± 0.05
Albumin (g/dl)	2.8 ± 0.17	2.4 ± 0.12	2.3 ± 0.05	2.3 ± 0.05	2.3 ± 0.12
Metabolites/hormones (n = 6)					
Triglyceride (mg/dl)	57 ± 4**	92 ± 13**	38 ± 8.2	27 ± 1.4	33.6 ± 3.2
NEFA (meq/liter)	1.7 ± 0.09**	1.7 ± 0.26*	1.0 ± 0.2	0.89 ± 0.09	0.92 ± 0.05
Glucose (mg/dl)	70 ± 14**	68 ± 17**	236 ± 25	296 ± 23*	236 ± 14
Insulin (ng/ml)	0.47 ± 0.08				0.52 ± 0.03
Glucagon (pg/ml)	>400**				37 ± 4.1
Liver (n = 6): triglyceride (mg/g)	182 ± 28.7**	133 ± 19**	22 ± 7*	13 ± 2	10 ± 1

[a] Abbreviations: AST, aspartate aminotransferase; ALT, alanine aminotransferase; ALP, alkaline phosphatase; NEFA, nonesterified free fatty acids.
[b] Statistically significant differences from Cre⁻ wild-type control are indicated by asterisks (*, $P < 0.05$; **, $P < 0.001$).

Metabolic characterization of albumin-Vhlh mutant mice demonstrated that the development of steatosis was associated with a significant elevation in serum transaminases and total bilirubin, indicating cellular liver damage and cholestasis (Table 1). In addition, albumin-Vhlh and -Vhlh/Hif-1α mutant mice developed hypoglycemia characterized by a 70% decrease in fasting glucose levels compared to those of wild-type littermate control mice. Glucagon levels were increased by greater than 10-fold in Vhlh mutant mice, and nonesterified free fatty acid levels were significantly elevated (Table 1). Lipid profile analysis of Vhlh-deficient mouse livers revealed that free cholesterol, cholesterol esters, diacylglycerol, and triacylglycerol levels were all significantly increased, with triacylglycerol levels being most dramatically affected (~13.5-fold increase [Table 2]). Analysis of total fatty acid composition did not indicate a chain length-dependent increase in fatty acids (examined were $C_{14:0}$, $C_{16:0}$, $C_{16:1n7}$, $C_{18:0}$, $C_{18:1n7}$, and $C_{20:0}$ [Table 2]). In contrast to Vhlh and Vhlh/Hif-1α mutants, all biochemical parameters analyzed in Vhlh/Hif-2α mutants, with the exception of a 2.2-fold increase in hepatic lipid content, were not statistically different from those of wild-type mice, demonstrating a central role for HIF-2 in the development of severe steatosis and hypoglycemia in Vhlh-deficient mouse livers (Table 1).

TABLE 2. Metabolic characterization of albumin-Cre mutant mice: hepatic lipid profile

Hepatic lipid(s) (unit of measure)	Mean ± SEM for mouse type[b]:	
	Vhlh	Cre⁻
FFA[a] (nmol/g)	5,632 ± 243	4,927 ± 436
Free cholesterol (nmol/g)	8,940 ± 351**	5,037 ± 94
Cholesterol esters (nmol/g)	6,341 ± 792**	2,365 ± 171
Phospholipid (nmol/g)	21,100 ± 433**	38,658 ± 619
Diacylglycerol (nmol/g)	3,360 ± 289**	1,301 ± 194
Triacylglycerol (nmol/g)	236,300 ± 17,372**	17,405 ± 3,813
$C_{14:0}$ (nmol/g)	40,204 ± 3,986**	1,130 ± 280
$C_{16:0}$ (nmol/g)	192,304 ± 11,056**	13,274 ± 3,068
$C_{16:1n7}$ (nmol/g)	15,770 ± 1,397**	1,325 ± 342
$C_{18:0}$ (nmol/g)	27,910 ± 3,199**	1,239 ± 237
$C_{18:1n7}$ (nmol/g)	9,824 ± 360**	847 ± 155
$C_{20:0}$ (nmol/g)	889 ± 130**	54.5 ± 11

[a] FFA, free fatty acids.
[b] Statistically significant differences from Cre⁻ wild-type control are indicated by asterisks (**, $P < 0.001$).

Lipogenic gene expression is suppressed in Vhlh mutant mouse livers. To investigate the molecular mechanisms underlying the development of Hif-2-mediated steatosis in Vhlh-deficient mice, we utilized cDNA microarrays enriched for genes expressed in the liver. We specifically focused on metabolic genes that were differentially expressed between Vhlh/Hif-1α mutant (increased Hif-2 activity) and Vhlh/Hif-1α/Hif-2α-deficient mouse livers (control liver without Hif stabilization). In addition, we analyzed gene expression profiles in Vhlh/Hif-2α (increased Hif-1 activity) and Vhlh/Hif-1α/Hif-2α mutant mouse livers to identify genes that were regulated in a Hif-1-dependent manner. Differentially expressed genes (>1.5-fold change) were grouped into functional categories that covered lipid, carbohydrate, oxygen, reactive oxygen species, energy, and pyruvate metabolism. Using these criteria, we identified 16 genes that were significantly induced between Vhlh/Hif-2α- and Vhlh/Hif-1α/Hif-2α-deficient mouse livers, which included *enolase 1* (*Eno1*) and *lactate dehydrogenase 1* (*Ldh1*/*Ldha*), suggesting Hif-1-dependent regulation of glycolysis and pyruvate metabolism (Fig. 2A; see also Fig. S2 in the supplemental material). One hundred fifty-seven genes were differentially expressed between Vhlh/Hif-1α and Vhlh/Hif-1α/Hif-2α mutant mouse livers (Fig. 2B and C).

Functional pathway analysis of genes differentially expressed in a Hif-2-dependent manner indicated that the Srebp-1c signaling pathway was significantly downregulated in Vhlh-deficient mouse livers. Srebp-1c is a sterol regulatory element binding protein that plays a central role in the regulation of lipid metabolism by stimulating de novo lipogenesis. In transgenic mice, forced Srebp-1c expression stimulates lipogenesis and results in the development of hepatic steatosis (47, 48). cDNA microarray and real-time PCR

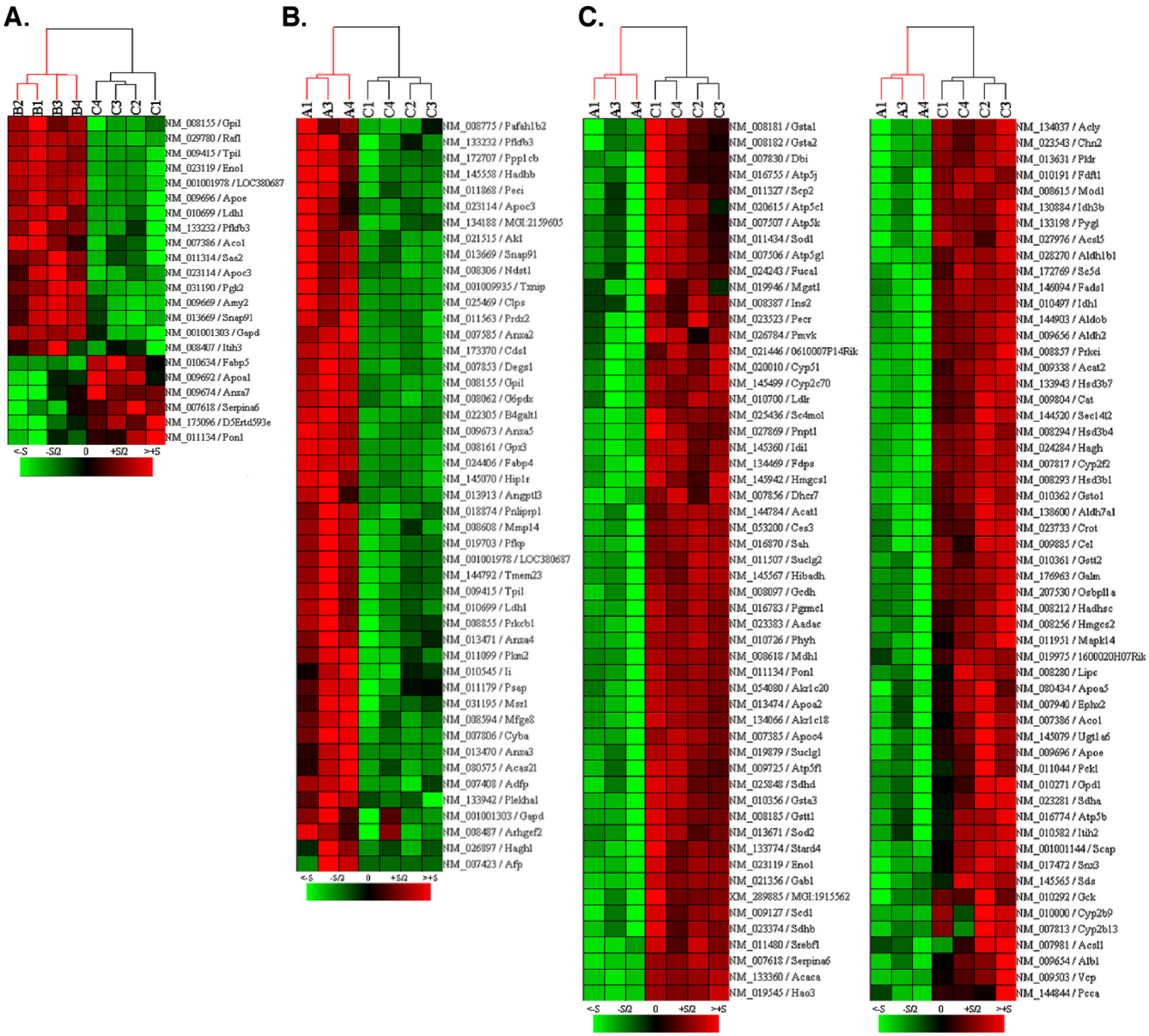

FIG. 2. Hierarchical cluster analysis of Hif-2-dependent metabolic gene expression in the liver. Shown are differentially regulated genes that were upregulated or downregulated 1.5-fold or greater in albumin-Vhlh mutant mouse livers in a Hif-1 (A)- or a Hif-2 (B and C)-dependent manner. Genes@Work (IBM) was used to generate a heat map depicting gene expression levels in albumin-Vhlh/Hif-1α/Hif-2α (group C, $n = 4$; triple mutant with absent Hif signaling), -Vhlh/Hif-2α (group B, $n = 4$; double mutant with active Hif-1), and -Vhlh/Hif-1α (group A, $n = 3$; double mutant with active Hif-2) mutant mouse livers compared to a common reference RNA sample. Red and green boxes represent an increase or decrease in expression, respectively. Each column represents expression levels in an individual liver sample. Genes were clustered using Euclidean average linkage clustering.

analysis revealed a significant decrease in *sterol regulatory element binding factor 1* (*Srebpf1*) and *Srebp cleavage-activating protein* (*Scap*), as well as the Srebp targets *Ldlr* and *Hmgcs1* in albumin-Vhlh/Hif-1α and -Vhlh mutant mouse livers (Fig. 3A). Importantly, we also observed a significant decrease in two of the key Srebp-1c targets that control lipogenesis, including *fatty acid synthase* (*Fasn*) and *acetyl-CoA carboxylase* (*Acc*) (Fig. 3B and C) (26, 27). Taken together, these results suggest that the development of steatosis in Vhlh mutant mice was not a consequence of increased lipid synthesis.

Activation of Hif-2α suppresses fatty acid β-oxidation in Vhlh-deficient mouse livers. Because the development of steatosis in Vhlh-deficient mice was not associated with increased lipogenesis, we next examined whether fatty acid β-oxidation was impaired in Vhlh mutant mice. We initially observed that the expression of peroxisome proliferator-activated receptor α (PPARα) targets, including *Hmgcs2*, *Apoa2*, *Apoa5*, *Acsl1*, and *Scd1* (28), was significantly decreased in albumin-Vhlh/Hif-1α mouse livers compared to -Vhlh/Hif-1α/Hif-2α-deficient mouse livers by microarray analysis, suggesting that PPARα signaling

A.

Gene	Entrez Gene ID	Description	Avg. Fold Induction	Verified
Srebf1	20787	sterol regulatory element binding factor 1	−1.63	YES
Scap	235623	SREBP cleavage activating protein	−1.87	YES
Ldlr	16835	low density lipoprotein receptor	−2.48	YES
Hmgcs1	208715	3-hydroxy-3-methylglutaryl-Coenzyme A synthase 1	−2.48	N/D

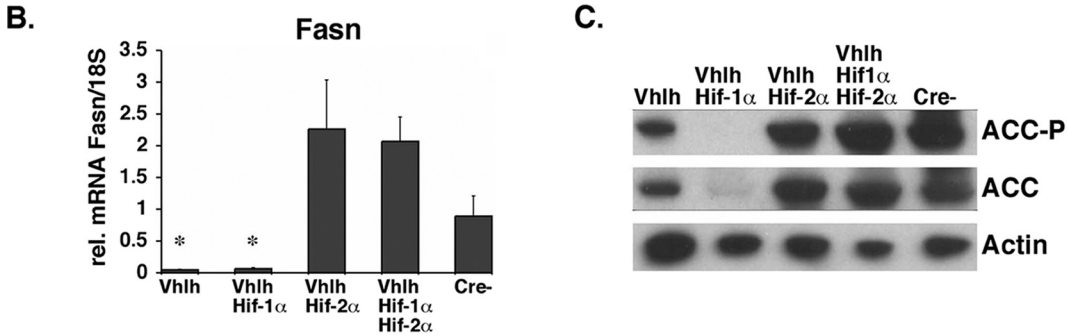

FIG. 3. Srebp-1c and lipogenic gene expression is suppressed in albumin-Vhlh mutant mouse livers. (A) List of genes in the Srebp-1c signaling pathway that are differentially expressed between albumin-Vhlh/Hif-1α and -Vhlh/Hif-1α/Hif-2α mutant mouse livers determined by microarray analysis. Microarray results were confirmed by real-time PCR analysis where indicated. N/D, not determined. (B) Real-time PCR analysis of *Fasn* expression in albumin-Cre mutant mouse livers. Relative expression levels were normalized to 18S. Error bars represent the standard errors of the means ($n = 4$). Asterisks indicate a statistically significant decrease in *Fasn* expression compared to control mice as determined by the Student *t* test (*, $P < 0.05$). (C) Western blot analysis of acetyl-CoA carboxylase (ACC) and phosphorylated ACC (ACC-P) protein levels in albumin-Cre mutant mouse cytoplasmic liver extracts. Actin was used as a protein loading control.

was impaired in mutant mouse livers (Fig. 4A). It is well established that PPARα is a central regulator of fatty acid metabolism through its transcriptional control of key enzymes involved in β-oxidation (for a review, see reference 23). Therefore, we investigated mRNA levels of individual PPARα target genes involved in fatty acid β-oxidation by real-time PCR. We found that the expression of acyl-CoA synthase long-chain family member 1 (Acsl1), which catalyzes one of the first steps of fatty acid oxidation (43), and *carnitine-palmitoyltransferase I* (*Cpt-1*), which controls mitochondrial fatty acid import (9, 24), was significantly suppressed in albumin-Vhlh and -Vhlh/Hif-1α mutant mouse livers (Fig. 4B). In addition, PPARα targets *acyl-CoA oxidase* (*Aco*) and *carnitine O-octanoyltransferase* (*Crot*) (9, 24, 50), which control peroxisomal β-oxidation, were downregulated (Fig. 4C). Inactivation of Hif-2α in albumin-Vhlh mutants restored *Acsl-1*, *Cpt1*, *Aco*, and *Crot* expression to control levels (Fig. 4B and C). Taken together, these data suggest that the development of hepatic steatosis in Vhlh mutant mice is associated with a Hif-2-dependent decrease in fatty acid β-oxidation.

To provide functional evidence that β-oxidation is specifically affected, we determined substrate oxidation rates in mitochondria isolated from albumin-Vhlh and control mouse livers. The rates of ADP-stimulated oxygen consumption with substrates including palmitoylcarnitine, octanoylcarnitine, and acetylcarnitine were determined using polarographic measurements. A statistically significant decrease in state 3 oxygen consumption was observed in Vhlh-deficient mitochondria for palmitoylcarnitine (Fig. 4D), suggesting that fatty acid β-oxidation was functionally impaired. In addition, fatty acid β-oxidation in mitochondria isolated from Vhlh-deficient mouse livers could not be restimulated by the addition of fresh ADP (data not shown). Normally, oxygen consumption diminishes when most of the ADP has been converted to ATP and then can be restimulated by the addition of fresh ADP. When carnitine esters were used as substrates, the addition of fresh ADP did not restimulate oxygen consumption to prior levels in Vhlh-deficient mitochondria, indicating a significant functional defect in fatty acid β-oxidation (data not shown). To determine if the mitochondrial respiratory chain was impaired, we examined oxygen consumption rates for Krebs cycle intermediates. No statistical difference in oxygen consumption rates was observed between Vhlh and control mutants when glutamate and succinate were used as substrates (data not shown). These findings indicate that mitochondria isolated from Vhlh mutant mice can oxidize other substrates with normal efficiency and that oxidative phosphorylation in Vhlh-deficient mitochondria itself is not affected. Taken together, our data suggest that inactivation of Vhlh in hepatocytes results in a Hif-2-dependent mitochondrial β-oxidation defect, which may have contributed to the development of hepatic steatosis.

Inactivation of Hif-2α restores gluconeogenic gene expression. To investigate the mechanisms underlying the development of hypoglycemia in *Vhlh*-deficient mice, we examined the expression of enzymes critical for hepatic gluconeogenesis. Real-time PCR analysis revealed that *phosphoenolpyruvate-carboxykinase* (*Pepck*) and *glucose-6-phosphatase* (*G6Pase*) mRNA levels were significantly decreased (Fig. 5). While inactivation of Hif-1α did not improve serum glucose levels or gluconeogenic gene expression, inactivation of Hif-2α restored gluconeogenic gene expression and rescued the hypoglycemic phenotype of Vhlh mutants (Fig. 5 and Table 1). Given the suppressive role of insulin signaling in gluconeogenesis, we next examined whether enhanced insulin signaling may have contributed to the development of hypoglycemia in Vhlh mutants. We did not observe changes in S473-phosphorylated Akt or S9-phosphorylated Gsk3β levels, suggesting that increased insulin sensitivity was not a contributing factor to this phenotype (data not shown). However, we found

A.

Gene	Entrez Gene ID	Description	Avg. Fold Induction	Verified
Hmgcs2	15360	3-hydroxy-3-methylglutaryl-Coenzyme A synthase 2	-1.95	YES
Apoa2	11807	apolipoprotein A-II	-4.04	YES
Apoa5	66113	apolipoprotein A-V	-2.29	YES
Acsl1	14081	acyl-CoA synthetase long-chain family member 1	-1.74	YES
Acsl5	433256	acyl-CoA synthetase long-chain family member 5	-1.96	N/D
Scd1	20249	stearoyl-Coenzyme A desaturase 1	-4.59	YES

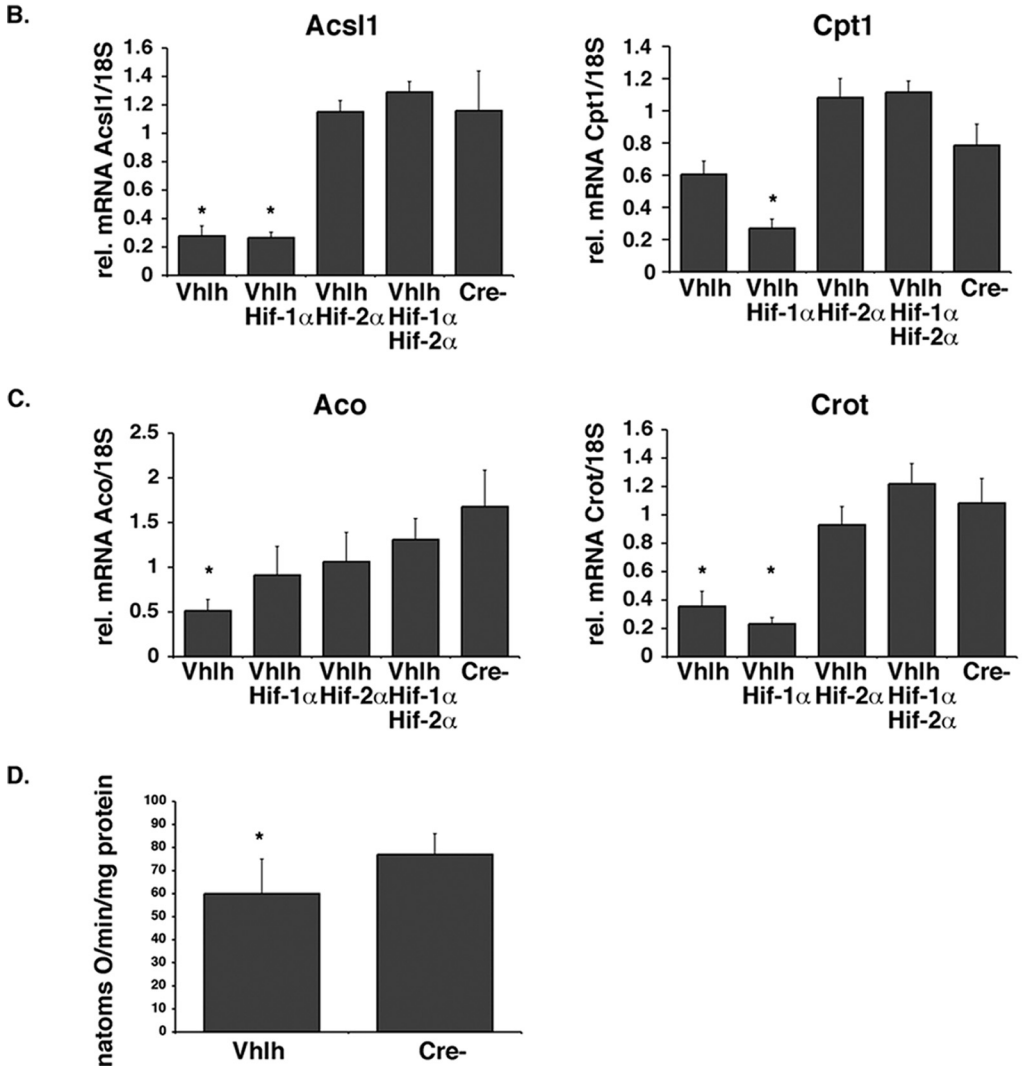

FIG. 4. Inactivation of Hif-2α restores fatty acid β-oxidation gene expression in albumin-Vhlh mutant mouse livers. (A) List of PPARα target genes that are differentially expressed between albumin-Vhlh/Hif-1α and -Vhlh/Hif-1α/Hif-2α mutant mouse livers as determined by microarray analysis. Microarray results were confirmed by real-time PCR analysis where indicated. (B and C) Quantitative real-time PCR analysis of PPARα target genes and key enzymes involved in mitochondrial (B) and peroxisomal (C) β-oxidation. Shown are average mRNA transcript levels for each genotype; error bars represent standard errors of the means ($n = 4$). Asterisks indicate a statistically significant difference in gene expression compared to control mice (Cre^-) as determined by the Student t test (*, $P < 0.05$; **, $P < 0.001$). Abbreviations: Acsl1, acyl-CoA synthase long-chain family member 1; Cpt1, carnitine-palmitoyltransferase I; Aco, acyl-CoA oxidase; Crot, carnitine *O*-octanoyltransferase. (D) State 3 oxygen consumption rates for palmitoylcarnitine in isolated mitochondria from albumin-Vhlh (Vhlh) and control (Cre^-) mutant mouse livers. For panels B to D, asterisks indicate a statistically significant decrease in oxygen consumption compared to control mice (Cre^-) as determined by the Student t test (*, $P < 0.05$). Error bars represent standard errors of the means ($n = 5$).

that *peroxisome proliferator-activated receptor γ coactivator 1α* (*Pgc-1α*) and *hepatocyte nuclear factor 4* (*Hnf4*), which are both key modulators of hepatic gluconeogenesis (40, 54), were significantly decreased. Therefore, it may be possible that activation of Hif-2 suppresses gluconeogenesis through direct or indirect regulation of one or both of these factors (Fig. 4). In addition to its role in gluconeogenesis, Pgc-1α enhances the activity of PPARα, and its downregulation is consistent with a transcriptional suppression of PPARα-dependent target genes that we have observed (Fig. 4).

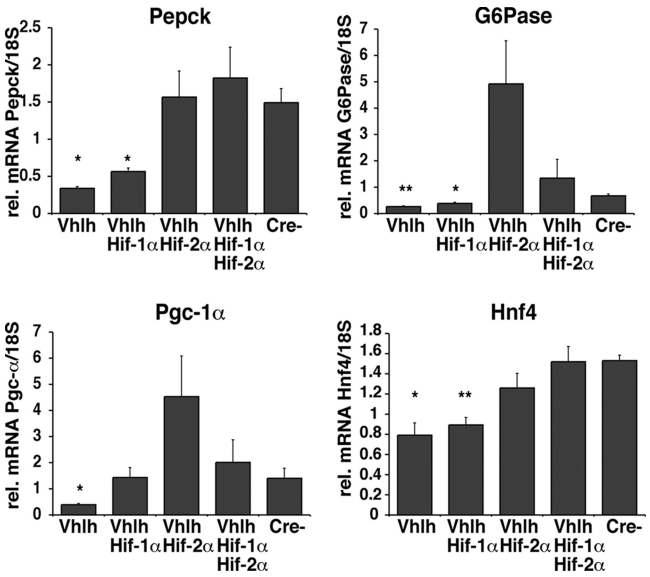

FIG. 5. Inactivation of Hif-2α restores gluconeogenic gene expression in albumin-Vhlh mutant mouse livers. Relative expression levels of gluconeogenic genes in the livers of 4-week-old albumin-Cre mutant mice determined by real-time PCR. Expression levels were normalized to 18S. Shown are the average mRNA expression levels for each genotype; error bars represent standard errors of the means ($n = 4$). Asterisks indicate a statistically significant change in gene expression compared to control as determined by the Student t test (*, $P < 0.05$; **, $P < 0.001$).

Hif-2 regulates fatty acid-storing capability in hepatocytes. Having determined that Vhlh deficiency in hepatocytes results in a significant defect in mitochondrial fatty acid β-oxidation and that Hif-2α is required for the development of hepatocellular steatosis, we sought to identify additional Hif-2-mediated processes that might contribute to the pathogenesis of this phenotype. Microarray analysis identified the gene encoding the lipid droplet binding protein adipose differentiation-related protein (*Adfp*) as a significantly upregulated gene in Vhlh-deficient mouse livers (Fig. 2). Adfp has previously been shown to be a critical regulator of lipid homeostasis in multiple cell types. Notably, Adfp is required and sufficient for cellular lipid accumulation in fibroblasts and models of fatty liver disease (4, 14, 15). Real-time PCR and Western blot analysis revealed that Adfp was significantly increased in both Vhlh and Vhlh/Hif-1α mutant mouse livers but not in Vhlh/Hif-2α-deficient mouse livers (Fig. 6A and B). Immunofluorescence localized Adfp (red) to macrovesicular lipid droplets, which are found throughout the livers of albumin-Vhlh and -Vhlh/Hif-1α mutant mice (Fig. 6C). We also stained PEPCK-Vhlh-deficient livers for Adfp and lipids. In contrast to albumin-Cre, which targets the majority of hepatocytes (80 to 90%), PEPCK-Cre targets only a subset of hepatocytes (~20 to 30%), which are predominantly localized in periportal areas (36). Although PEPCK-Vhlh mutant mice developed vascular lesions associated with focal hepatic steatosis, as indicated by the presence of Adfp-positive macrovesicular lipid droplets (Fig. 6D), mice had normal serum transaminase values and normal serum metabolic parameters (36; also data not shown), supporting the notion that lipid accumulation is a cell-autonomous consequence of *Vhlh* deletion in hepatocytes rather than the result of serum and/or systemic metabolic abnormalities found in albumin-Cre mutants (Table 1).

We next sought to determine if increased Adfp expression in Vhlh-deficient mouse livers is a direct result of enhanced Hif activity or secondary to lipid accumulation. To test this, we first examined *ADFP* mRNA levels in human HepG2 hepatoma cells that were exposed to 1% oxygen for 16 h. Real-time PCR analysis showed that *ADFP* was significantly upregulated following exposure to hypoxia (Fig. 6E). Using siRNA-mediated knockdown of *HIF-1α*, *HIF-2α*, and *ARNT*, we found that the hypoxic induction of *ADFP* was largely dependent on intact HIF signaling (*ARNT* knockdown) and appeared to be preferentially mediated by HIF-2 (Fig. 6E). This suggested that increased Adfp levels in Vhlh mutant mice are primarily the result of Hif activation rather than a consequence of neutral fat accumulation. Further evidence in support of this notion was provided by comparison of the expression of Adfp with that of other lipid binding proteins, including perilipin A (Plin), mannose-6-phosphate receptor binding protein 1 (M6prbp1, also known as Tip47), and plasma membrane-associated protein (Pmap; the human orthologue is known as S3-12) in hypoxic hepatocytes and Vhlh-deficient mouse livers (32). We observed that Adfp was the only lipid binding protein that was significantly induced in both Vhlh-deficient mouse fatty livers and hypoxic hepatocytes (Fig. 6F), indicating that increased expression of Adfp may be an early and initiating event in the pathogenesis of Hif-2-mediated hepatocellular steatosis. Taken together, our data suggest that Hif-2-mediated increased Adfp expression may have contributed to the development of hepatic steatosis in Vhlh-deficient mouse livers.

DISCUSSION

In this report we characterized a genetic model of VHL-associated hepatocellular steatosis and identified HIF-2 as a central regulator of hepatic lipid metabolism. We found that activation of HIF-2 resulted in suppression of fatty acid β-oxidation and lipid synthesis as well as an increase in lipid storage capability. We propose that, in this model, HIF-2 controls at least three components of hepatic lipid metabolism: synthesis, oxidation, and storage.

Cells adapt metabolically to hypoxia by switching from aerobic to anaerobic metabolism in order to generate ATP in an oxygen-independent manner. This process, known as the Pasteur effect, is the result of increased glucose uptake and glycolysis, as well as decreased mitochondrial oxidative phosphorylation (44). HIF-1 plays a central role in this process as it regulates the switch from pyruvate catabolism and oxidative phosphorylation to glycolysis in both hypoxic and normoxic (e.g., VHL-deficient) cells (Fig. 7). HIF-1 directly stimulates glycolysis by activating the expression of glucose transporters and glycolytic enzymes (12, 19, 55) and inhibits mitochondrial oxidative phosphorylation by blocking pyruvate entry and conversion to acetyl-CoA in the mitochondria through activation of pyruvate dehydrogenase kinase, a negative regulator of pyruvate dehydrogenase activity (33). Recent studies have shown that HIF-1 can also indirectly repress mitochondrial metabolism and biogenesis by antagonizing c-Myc activity (55). While these findings explain the effects of low oxygen on glu-

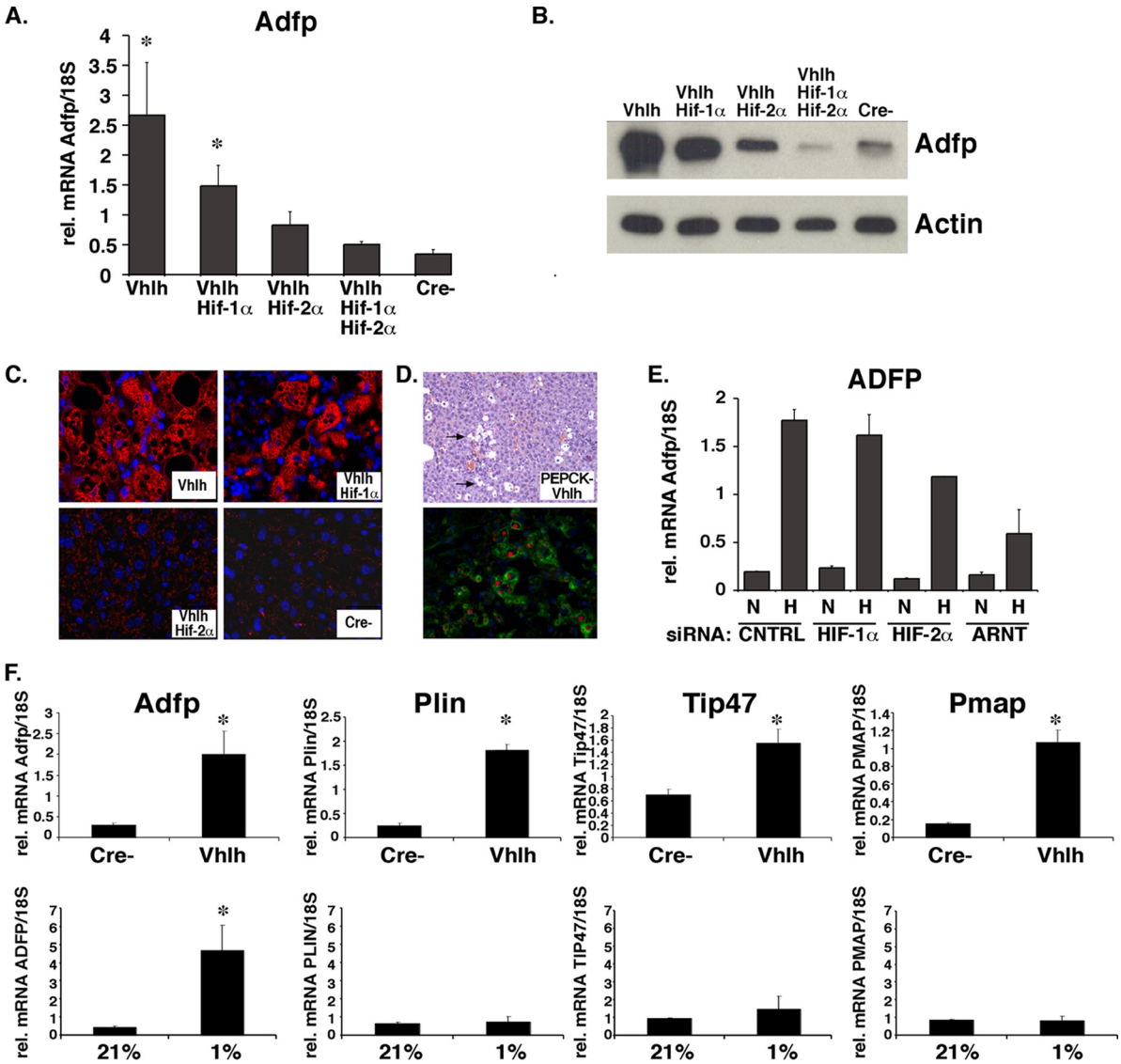

FIG. 6. Adfp is preferentially regulated by Hif-2α in hepatocytes. (A) Real-time PCR analysis of *Adfp* expression in albumin-Cre mutant mouse livers. Expression levels were normalized to 18S. Shown are the average mRNA expression levels for the indicated genotypes; error bars represent standard errors of the means ($n = 3$). Asterisks indicate a statistically significant change in gene expression compared to control as determined by the Student t test (*, $P < 0.05$). (B) Western blot analysis of Adfp expression in albumin-Cre mutants. Cytoplasmic protein extracts were used for analysis. Actin served as a loading control. (C) Immunofluorescent staining for Adfp (red) in albumin-Cre mutant mouse liver sections counterstained with 4′,6-diamidino-2-phenylindole (blue nuclei). (D) Hematoxylin and eosin (top) and immunofluorescent (bottom) staining for Adfp (green) and Nile red (red) in PEPCK-Vhlh mutant mouse liver sections. Arrows point to areas of hepatic steatosis. (E) Real-time PCR analysis of *ADFP* expression in normoxic (N) and hypoxic (H; 16 h, 1% O_2) HepG2 cells treated with control, *HIF-1α*, *HIF-2α*, or *ARNT* siRNA oligonucleotides. (F) Real-time PCR analysis of lipid droplet binding protein expression in albumin-Cre mutant mouse livers (top) and HepG2 cells exposed to 21% or 1% oxygen for 16 h (bottom). Expression levels were normalized to 18S. Bars represent the mean mRNA expression levels of four samples per group; error bars represent standard errors of the means. Asterisks indicate a statistically significant change in gene expression compared to control as determined by the Student t test (*, $P < 0.05$).

cose and pyruvate metabolism, the regulation of lipid metabolism under hypoxic conditions is not well understood. The identification of underlying molecular mechanisms would be particularly relevant for tissues such as liver, lung, and heart, where fatty acids are the preferred carbon source for the generation of ATP. In these tissues, hypoxia results in suppressed fatty acid oxidation and neutral lipid accumulation (5, 13, 21, 30, 53). In this report, we have generated a model of constitutive HIF activation in the liver and demonstrate that HIF-2, but not HIF-1, suppresses fatty acid oxidation and promotes lipid accumulation (Fig. 7). These findings indicate that HIF-2 is the predominant HIF for the regulation of lipid metabolism.

Our findings demonstrate that activation of HIF-2 alters hepatic lipid metabolism and results in the development of severe fatty liver disease in mice. The phenotype in our model resembles that found in patients with nonalcoholic fatty liver disease (NAFLD), which raises the possibility that HIF-2 may contribute to the development of this disease. NAFLD is char-

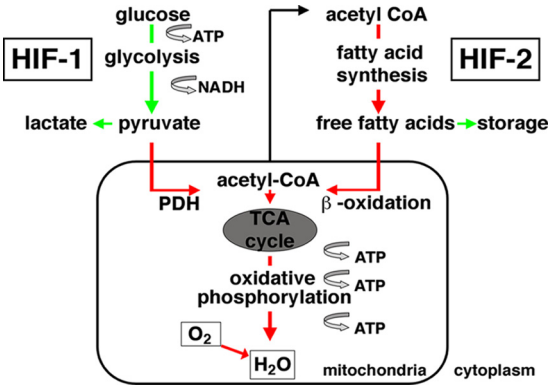

FIG. 7. Model depicting the roles of HIF-1 and HIF-2 in the regulation of hepatic glucose and lipid metabolism. Cells adapt metabolically to hypoxia by switching from aerobic to anaerobic metabolism in order to generate ATP in an oxygen-independent manner. While HIF-1 regulates glycolysis and pyruvate metabolism, HIF-2 controls fatty acid metabolism. Together, HIF-1 and HIF-2 cooperate in the reprogramming of metabolic pathways to generate cellular energy when oxidative phosphorylation is impaired due to decreased availability of molecular oxygen. Red lines indicate inhibitory effects of HIF activation; stimulatory effects of HIF activation are indicated by green arrows.

acterized by fat accumulation in hepatocytes and can be associated with inflammation (nonalcoholic steatohepatitis) or fibrosis (2). Nonalcoholic steatohepatitis may progress to cirrhosis in up to 20% of patients and represents a leading cause of cryptogenic cirrhosis. Insulin resistance, oxidative injury, iron, and antioxidant deficiencies among other factors have been implicated in the pathogenesis of NAFLD, which is still poorly understood. Chronic sleep apnea has been associated with fatty livers, suggesting that liver hypoxia, which activates HIF-2, may be a contributory factor (49). Furthermore, it has been suggested that hypoxia contributes to the development of steatosis in patients with alcohol-induced liver damage and heart failure (17). In addition to NAFLD, our findings have relevance for patients with VHL disease. Similar to the genetic model utilized in this study, patients with germ line mutations in the VHL tumor suppressor develop tumors that accumulate lipids. Most notably, VHL-associated renal cell carcinomas are distinguished histologically from other types of renal cancer by the presence of a "clear" cytoplasm, which results from the washout of lipids during tissue processing. Furthermore, lipid accumulation is a characteristic of stromal cells, which are the neoplastic components of VHL-associated hemangioblastomas (20). Thus, our studies identify HIF-2 as a molecular mediator of the clear-cell phenotype that is a morphological hallmark of VHL-associated neoplasms.

Excess lipid accumulation in the liver and the development of NAFLD can result from increased lipid synthesis or from a decrease in the ability to oxidize fatty acids (2). With regard to VHL-associated heptocellular steatosis, we established that key lipogenic enzymes, such as FASN and ACC, were significantly downregulated in a HIF-2-dependent manner. In addition, we also observed a HIF-2-dependent suppression of FASN expression in hypoxic HepG2 cells (see Fig. S3 in the supplemental material). These findings suggest that HIF-2-mediated lipid accumulation was not a result of increased lipid synthesis. Instead, using polarographic measurements of oxygen consumption, we found a functional decrease in the ability of pVHL-deficient hepatocytes to oxidize fatty acids. Furthermore, gene expression analysis of pVHL-deficient mouse livers suggested a functional interaction between HIF and nuclear hormone receptor signaling through PPARα, a central regulator of fatty acid oxidation and gluconeogenesis (22, 39). The importance of PPARα in maintaining hepatic energy balance is illustrated by the findings that PPARα-deficient mice develop steatohepatitis and hypoglycemia (18). We found that a number of PPARα targets, including those which control β-oxidation (*Acsl1* and *Cpt1*), were decreased by HIF-2 in pVHL-deficient mouse livers and renal cell carcinoma cells (see Fig. S3 in the supplemental material). Whether HIF-2 has a direct or indirect role in suppressing PPARα transcriptional activity requires further investigation. HIF-1 has been shown to directly inhibit PPARα expression in intestinal and oral epithelial cells (31); however, we did not observe a significant decrease in PPARα protein levels in pVHL-deficient mouse livers (data not shown). PPARα activity may also be indirectly suppressed through a decrease in lipogenesis. Using a mouse model of liver-specific Fas knockdown, Chakravarthy et al. demonstrated that de novo lipid synthesis is required to activate PPARα and stimulate β-oxidation in the liver (3). This raises the possibility that HIF-2 may regulate β-oxidation indirectly through its suppressive effects on lipogenesis. Future studies are needed to further explore the role of HIF-2 in the regulation of hepatic PPARα signaling.

In addition to suppressed fatty acid oxidation in pVHL-deficient livers, we also observed increased expression of the lipid droplet binding protein ADFP, which may have contributed to the development of steatosis. ADFP is a member of the PAT family of lipid droplet binding proteins, which include perilipin A, TIP47, and Pmap (25), and plays an active role in regulating lipid stores in a variety of cell types. Overexpression of Adfp increased both the number and size of lipid droplets in murine fibroblasts, while inhibition of Adfp prevented the development of steatosis in leptin-deficient and diet-induced fatty liver models (4, 14, 15). We found that ADFP was induced by HIF-2 in hypoxic human hepatoma cells, indicating direct regulation by HIF-2, which is consistent with previous reports on pVHL-deficient renal cell carcinoma cells (12). While perilipin A, TIP47, and Pmap were also increased in fatty livers of Vhlh-deficient mice, ADFP was the only PAT family member that was hypoxia inducible, suggesting that ADFP may be an early and initiating event in the pathogenesis of HIF-2-mediated steatosis. Efforts are under way in our laboratory to examine the roles of ADFP and other PAT family members in the development of HIF-2-mediated steatosis.

In summary, we have shown that constitutive HIF-2 activation in hepatocytes results in the development of severe hepatic steatosis, which is associated with suppression of lipid synthesis and fatty acid β-oxidation, and an increase in lipid storage capacity. These findings demonstrate that efficient control of HIF-2 signaling is necessary to maintain normal lipid homeostasis in the liver and may have implications for the development of new therapeutic strategies aimed at the treatment of fatty liver diseases.

ACKNOWLEDGMENTS

This work was supported by NIH grants DK073467 and DK080821 and in part by NIH grant CA100787 (all to V.H.H.), by the Penn Center for Molecular Studies in Digestive and Liver Disease (P30-DK50306), and by the Penn Institute for Diabetes, Obesity, and Metabolism (P30-DK19525).

We thank Peter White and Klaus Kaestner for help with the microarray analysis, Rexford Ahima for help with the metabolic analysis, and Chia H. Wu for technical assistance.

We disclose that no financial conflict of interest exists.

REFERENCES

1. **Bruder, E. D., P. C. Lee, and H. Raff.** 2005. Lipid and fatty acid profiles in the brain, liver, and stomach contents of neonatal rats: effects of hypoxia. Am. J. Physiol. Endocrinol. Metab. **288:**E314–E320.
2. **Brunt, E. M., B. A. Neuschwander-Tetri, D. Oliver, K. R. Wehmeier, and B. R. Bacon.** 2004. Nonalcoholic steatohepatitis: histologic features and clinical correlations with 30 blinded biopsy specimens. Hum. Pathol. **35:** 1070–1082.
3. **Chakravarthy, M. V., Z. Pan, Y. Zhu, K. Tordjman, J. G. Schneider, T. Coleman, J. Turk, and C. F. Semenkovich.** 2005. "New" hepatic fat activates PPARalpha to maintain glucose, lipid, and cholesterol homeostasis. Cell Metab. **1:**309–322.
4. **Chang, B. H., L. Li, A. Paul, S. Taniguchi, V. Nannegari, W. C. Heird, and L. Chan.** 2006. Protection against fatty liver but normal adipogenesis in mice lacking adipose differentiation-related protein. Mol. Cell. Biol. **26:**1063–1076.
5. **Das, D. K., J. Ayromlooi, and A. Neogi.** 1983. Effect of ischemia on fatty acid metabolism in fetal lung. Life Sci. **33:**569–576.
6. **Folch, J., M. Lees, and G. H. S. Stanley.** 1957. A simple method for the isolation and purification of total lipids from animal tissues. J. Biol. Chem. **226:**497–509.
7. **Fukumoto, S., and T. Fujimoto.** 2002. Deformation of lipid droplets in fixed samples. Histochem. Cell Biol. **118:**423–428.
8. **Gruber, M., C. J. Hu, R. S. Johnson, E. J. Brown, B. Keith, and M. C. Simon.** 2007. Acute postnatal ablation of Hif-2alpha results in anemia. Proc. Natl. Acad. Sci. USA **104:**2301–2306.
9. **Gulick, T., S. Cresci, T. Caira, D. D. Moore, and D. P. Kelly.** 1994. The peroxisome proliferator-activated receptor regulates mitochondrial fatty acid oxidative enzyme gene expression. Proc. Natl. Acad. Sci. USA **91:**11012–11016.
10. **Haase, V. H., J. N. Glickman, M. Socolovsky, and R. Jaenisch.** 2001. Vascular tumors in livers with targeted inactivation of the von Hippel-Lindau tumor suppressor. Proc. Natl. Acad. Sci. USA **98:**1583–1588.
11. **Hamaguchi, T., N. Iizuka, R. Tsunedomi, Y. Hamamoto, T. Miyamoto, M. Iida, Y. Tokuhisa, K. Sakamoto, M. Takashima, T. Tamesa, and M. Oka.** 2008. Glycolysis module activated by hypoxia-inducible factor 1alpha is related to the aggressive phenotype of hepatocellular carcinoma. Int. J. Oncol. **33:**725–731.
12. **Hu, C. J., L. Y. Wang, L. A. Chodosh, B. Keith, and M. C. Simon.** 2003. Differential roles of hypoxia-inducible factor 1α (HIF-1α) and HIF-2α in hypoxic gene regulation. Mol. Cell. Biol. **23:**9361–9374.
13. **Huss, J. M., F. H. Levy, and D. P. Kelly.** 2001. Hypoxia inhibits the peroxisome proliferator-activated receptor alpha/retinoid X receptor gene regulatory pathway in cardiac myocytes: a mechanism for O2-dependent modulation of mitochondrial fatty acid oxidation. J. Biol. Chem. **276:**27605–27612.
14. **Imai, Y., G. M. Varela, M. B. Jackson, M. J. Graham, R. M. Crooke, and R. S. Ahima.** 2007. Reduction of hepatosteatosis and lipid levels by an adipose differentiation-related protein antisense oligonucleotide. Gastroenterology **132:**1947–1954.
15. **Imamura, M., T. Inoguchi, S. Ikuyama, S. Taniguchi, K. Kobayashi, N. Nakashima, and H. Nawata.** 2002. ADRP stimulates lipid accumulation and lipid droplet formation in murine fibroblasts. Am. J. Physiol. Endocrinol. Metab. **283:**E775–E783.
16. **Jungermann, K.** 1988. Metabolic zonation of liver parenchyma. Semin. Liver Dis. **8:**329–341.
17. **Jungermann, K., and T. Kietzmann.** 2000. Oxygen: modulator of metabolic zonation and disease of the liver. Hepatology **31:**255–260.
18. **Kersten, S., J. Seydoux, J. M. Peters, F. J. Gonzalez, B. Desvergne, and W. Wahli.** 1999. Peroxisome proliferator-activated receptor alpha mediates the adaptive response to fasting. J. Clin. Investig. **103:**1489–1498.
19. **Kim, J. W., I. Tchernyshyov, G. L. Semenza, and C. V. Dang.** 2006. HIF-1-mediated expression of pyruvate dehydrogenase kinase: a metabolic switch required for cellular adaptation to hypoxia. Cell Metab. **3:**177–185.
20. **Kim, W. Y., and W. G. Kaelin.** 2004. Role of VHL gene mutation in human cancer. J. Clin. Oncol. **22:**4991–5004.
21. **Kinnula, V. L., and I. Hassinen.** 1978. Effect of chronic hypoxia on hepatic triacylglycerol concentration and mitochondrial fatty acid oxidizing capacity in liver and heart. Acta Physiol. Scand. **102:**64–73.
22. **Koo, S. H., H. Satoh, S. Herzig, C. H. Lee, S. Hedrick, R. Kulkarni, R. M. Evans, J. Olefsky, and M. Montminy.** 2004. PGC-1 promotes insulin resistance in liver through PPAR-alpha-dependent induction of TRB-3. Nat. Med. **10:**530–534.
23. **Lefebvre, P., G. Chinetti, J. C. Fruchart, and B. Staels.** 2006. Sorting out the roles of PPAR alpha in energy metabolism and vascular homeostasis. J. Clin. Investig. **116:**571–580.
24. **Leone, T. C., C. J. Weinheimer, and D. P. Kelly.** 1999. A critical role for the peroxisome proliferator-activated receptor alpha (PPARalpha) in the cellular fasting response: the PPARalpha-null mouse as a model of fatty acid oxidation disorders. Proc. Natl. Acad. Sci. USA **96:**7473–7478.
25. **Londos, C., C. Sztalryd, J. T. Tansey, and A. R. Kimmel.** 2005. Role of PAT proteins in lipid metabolism. Biochimie **87:**45–49.
26. **Magana, M. M., S. H. Koo, H. C. Towle, and T. F. Osborne.** 2000. Different sterol regulatory element-binding protein-1 isoforms utilize distinct co-regulatory factors to activate the promoter for fatty acid synthase. J. Biol. Chem. **275:**4726–4733.
27. **Magana, M. M., and T. F. Osborne.** 1996. Two tandem binding sites for sterol regulatory element binding proteins are required for sterol regulation of fatty-acid synthase promoter. J. Biol. Chem. **271:**32689–32694.
28. **Mandard, S., M. Muller, and S. Kersten.** 2004. Peroxisome proliferator-activated receptor alpha target genes. Cell. Mol. Life Sci. **61:**393–416.
29. **Maynard, M. A., H. Qi, J. Chung, E. H. Lee, Y. Kondo, S. Hara, R. C. Conaway, J. W. Conaway, and M. Ohh.** 2003. Multiple splice variants of the human HIF-3alpha locus are targets of the von Hippel-Lindau E3 ubiquitin ligase complex. J. Biol. Chem. **278:**11032–11040.
30. **Moore, K. H., J. F. Radloff, F. E. Hull, and C. C. Sweeley.** 1980. Incomplete fatty acid oxidation by ischemic heart: beta-hydroxy fatty acid production. Am. J. Physiol. **239:**H257–H265.
31. **Narravula, S., and S. P. Colgan.** 2001. Hypoxia-inducible factor 1-mediated inhibition of peroxisome proliferator-activated receptor alpha expression during hypoxia. J. Immunol. **166:**7543–7548.
32. **Olofsson, S. O., P. Bostrom, L. Andersson, M. Rutberg, J. Perman, and J. Boren.** 2009. Lipid droplets as dynamic organelles connecting storage and efflux of lipids. Biochim. Biophys. Acta **1791:**448–458.
33. **Papandreou, I., R. A. Cairns, L. Fontana, A. L. Lim, and N. C. Denko.** 2006. HIF-1 mediates adaptation to hypoxia by actively downregulating mitochondrial oxygen consumption. Cell Metab. **3:**187–197.
34. **Postic, C., M. Shiota, K. D. Niswender, T. L. Jetton, Y. Chen, J. M. Moates, K. D. Shelton, J. Lindner, A. D. Cherrington, and M. A. Magnuson.** 1999. Dual roles for glucokinase in glucose homeostasis as determined by liver and pancreatic beta cell-specific gene knock-outs using Cre recombinase. J. Biol. Chem. **274:**305–315.
35. **Rankin, E. B., M. P. Biju, Q. Liu, T. L. Unger, J. Rha, R. S. Johnson, M. C. Simon, B. Keith, and V. H. Haase.** 2007. Hypoxia-inducible factor-2 (HIF-2) regulates hepatic erythropoietin in vivo. J. Clin. Investig. **117:**1068–1077.
36. **Rankin, E. B., D. F. Higgins, J. A. Walisser, R. S. Johnson, C. A. Bradfield, and V. H. Haase.** 2005. Inactivation of the arylhydrocarbon receptor nuclear translocator (Arnt) suppresses von Hippel-Lindau disease-associated vascular tumors in mice. Mol. Cell. Biol. **25:**3163–3172.
37. **Rankin, E. B., J. Rha, T. L. Unger, C. H. Wu, H. P. Shutt, R. S. Johnson, M. C. Simon, B. Keith, and V. H. Haase.** 2008. Hypoxia-inducible factor-2 regulates vascular tumorigenesis in mice. Oncogene **27:**5354–5358.
38. **Rankin, E. B., J. E. Tomaszewski, and V. H. Haase.** 2006. Renal cyst development in mice with conditional inactivation of the von Hippel-Lindau tumor suppressor. Cancer Res. **66:**2576–2583.
39. **Reddy, J. K., and T. Hashimoto.** 2001. Peroxisomal beta-oxidation and peroxisome proliferator-activated receptor alpha: an adaptive metabolic system. Annu. Rev. Nutr. **21:**193–230.
40. **Rhee, J., Y. Inoue, J. C. Yoon, P. Puigserver, M. Fan, F. J. Gonzalez, and B. M. Spiegelman.** 2003. Regulation of hepatic fasting response by PPAR-gamma coactivator-1alpha (PGC-1): requirement for hepatocyte nuclear factor 4alpha in gluconeogenesis. Proc. Natl. Acad. Sci. USA **100:**4012–4017.
41. **Ryan, H. E., M. Poloni, W. McNulty, D. Elson, M. Gassmann, J. M. Arbeit, and R. S. Johnson.** 2000. Hypoxia-inducible factor-1alpha is a positive factor in solid tumor growth. Cancer Res. **60:**4010–4015.
42. **Schofield, C. J., and P. J. Ratcliffe.** 2004. Oxygen sensing by HIF hydroxylases. Nat. Rev. Mol. Cell Biol. **5:**343–354.
43. **Schoonjans, K., M. Watanabe, H. Suzuki, A. Mahfoudi, G. Krey, W. Wahli, P. Grimaldi, B. Staels, T. Yamamoto, and J. Auwerx.** 1995. Induction of the acyl-coenzyme A synthetase gene by fibrates and fatty acids is mediated by a peroxisome proliferator response element in the C promoter. J. Biol. Chem. **270:**19269–19276.
44. **Seagroves, T. N., H. E. Ryan, H. Lu, B. G. Wouters, M. Knapp, P. Thibault, K. Laderoute, and R. S. Johnson.** 2001. Transcription factor HIF-1 is a necessary mediator of the Pasteur effect in mammalian cells. Mol. Cell. Biol. **21:**3436–3444.
45. **Semenza, G. L.** 1999. Regulation of mammalian O2 homeostasis by hypoxia-inducible factor 1. Annu. Rev. Cell Dev. Biol. **15:**551–578.
46. **Semenza, G. L., P. H. Roth, H. M. Fang, and G. L. Wang.** 1994. Transcriptional regulation of genes encoding glycolytic enzymes by hypoxia-inducible factor 1. J. Biol. Chem. **269:**23757–23763.
47. **Shimano, H., J. D. Horton, I. Shimomura, R. E. Hammer, M. S. Brown, and**

J. L. Goldstein. 1997. Isoform 1c of sterol regulatory element binding protein is less active than isoform 1a in livers of transgenic mice and in cultured cells. J. Clin. Investig. **99:**846–854.

48. **Shimomura, I., H. Shimano, B. S. Korn, Y. Bashmakov, and J. D. Horton.** 1998. Nuclear sterol regulatory element-binding proteins activate genes responsible for the entire program of unsaturated fatty acid biosynthesis in transgenic mouse liver. J. Biol. Chem. **273:**35299–35306.
49. **Tanne, F., F. Gagnadoux, O. Chazouilleres, B. Fleury, D. Wendum, E. Lasnier, B. Lebeau, R. Poupon, and L. Serfaty.** 2005. Chronic liver injury during obstructive sleep apnea. Hepatology **41:**1290–1296.
50. **Tugwood, J. D., I. Issemann, R. G. Anderson, K. R. Bundell, W. L. McPheat, and S. Green.** 1992. The mouse peroxisome proliferator activated receptor recognizes a response element in the 5′ flanking sequence of the rat acyl CoA oxidase gene. EMBO J. **11:**433–439.
51. **Wenger, R. H.** 2002. Cellular adaptation to hypoxia: O2-sensing protein hydroxylases, hypoxia-inducible transcription factors, and O2-regulated gene expression. FASEB J. **16:**1151–1162.
52. **White, P., J. E. Brestelli, K. H. Kaestner, and L. E. Greenbaum.** 2005. Identification of transcriptional networks during liver regeneration. J. Biol. Chem. **280:**3715–3722.
53. **Whitmer, J. T., J. A. Idell-Wenger, M. J. Rovetto, and J. R. Neely.** 1978. Control of fatty acid metabolism in ischemic and hypoxic hearts. J. Biol. Chem. **253:**4305–4309.
54. **Yoon, J. C., P. Puigserver, G. Chen, J. Donovan, Z. Wu, J. Rhee, G. Adelmant, J. Stafford, C. R. Kahn, D. K. Granner, C. B. Newgard, and B. M. Spiegelman.** 2001. Control of hepatic gluconeogenesis through the transcriptional coactivator PGC-1. Nature **413:**131–138.
55. **Zhang, H., P. Gao, R. Fukuda, G. Kumar, B. Krishnamachary, K. I. Zeller, C. V. Dang, and G. L. Semenza.** 2007. HIF-1 inhibits mitochondrial biogenesis and cellular respiration in VHL-deficient renal cell carcinoma by repression of C-MYC activity. Cancer Cell **11:**407–420.